

# A white-light Michelson interferometer in the visible and near infrared regions

Takao Fuji, Mariko Arakawa, Toshiaki Hattori, and Hiroki Nakatsuka<sup>a)</sup>  
*Institute of Applied Physics, University of Tsukuba, Tsukuba, Ibaraki 305-8573, Japan*

(Received 18 March 1998; accepted for publication 27 May 1998)

A white-light Michelson interferometer in the visible and near infrared regions is described which can obtain the cross-correlation interferogram between the incident light and the transmitted light through samples or optical components. By comparing the autocorrelation interferogram of the incident white light with the cross-correlation interferogram between the incident light and the transmitted light, we can obtain linear response functions of samples or optical components with femtosecond time resolution. Fourier analysis of the interferograms gives also the complex optical constants of the samples without relying on the Kramers–Kronig relation. © 1998 American Institute of Physics. [S0034-6748(98)03408-X]

## I. INTRODUCTION

Fourier transform spectrometers (FTS), which are common in infrared regions, use Michelson interferometers. But in almost all the commercially available FTSs the sample is inserted behind the output end of the Michelson interferometer, and the autocorrelation interferogram of the transmitted light through the sample is obtained. To measure both the absorption spectrum and the spectrum of the refractive index, or the linear response function, of the sample, we have to insert the sample into only one arm of the Michelson interferometer and obtain not only the autocorrelation interferogram of the incident light but also the cross-correlation interferogram between the incident light and the transmitted light through the sample.<sup>1–7</sup> In the linear regime, by comparing the autocorrelation and the cross-correlation interferograms, we can obtain the response function and then predict the deformation of the pulse wave form by the passage through the sample. That is, if the wave form of the incident light pulse is the autocorrelation interferogram, then the wave form of the transmitted light is the cross-correlation interferogram as is shown below by using linear response theory. This means that the broad-spectral white-light Michelson interferometer can predict the wave form deformation of ultrashort light pulses by the passage through samples or optical components with very-high time resolution.<sup>8,9</sup> This information is very important for femtosecond laser technology and femtosecond spectroscopy.

In the Michelson interferometer, the two beams through the two arms of the interferometer must interfere with each other with a fixed phase relation throughout the beam cross section. This is easy for spatially coherent light such as a laser beam. But if the incident light is a spatially incoherent ordinary lamp, it becomes quite difficult especially in short-wavelength regions. Moreover if a sample is inserted in only one arm of the Michelson interferometer to obtain cross-correlation interferograms, the alignment becomes much more difficult. This is considered to be the reason why FTSs

which can obtain cross-correlation interferograms in the visible wavelength region are not commonly used. In the present article we describe a white-light Michelson interferometer which can obtain not only the autocorrelation interferogram but also the cross-correlation interferogram in the visible and near infrared regions.

## II. EXPERIMENTAL SYSTEM

A schematic diagram of the experimental system is shown in Fig. 1. The incident light source to the Michelson interferometer was a conventional incandescent lamp (halogen lamp) with a power consumption of 650 W which is normally used in a slide projector. The unpolarized light from the lamp was guided to a vibration-isolated bench through a multimode optical fiber with a core diameter of 0.8 mm (Sumitomo Electric, MK-08), and passed through a spatial filter composed of a microscope objective lens (20×) and a pinhole (100  $\mu\text{m}\phi$ ). The spatial filter was used to cut just the outermost part of the output light from the multimode fiber. The collimated light from the spatial filter with a beam diameter of 2 mm was guided to the Michelson interferometer composed of a nonpolarizing beam-splitter cube and two corner-cube prisms. Since the light source is an incoherent incandescent lamp, and the coherence area is much smaller than the beam cross section, we need to make fine adjustments in the order of a  $\mu\text{m}$  so that the same coherence areas of the two beams from the both arms overlap spatially. The obtained maximum interference depth was about 80%. Naganuma *et al.*<sup>2</sup> used a single mode fiber with a core diameter of about 3  $\mu\text{m}$  to obtain spatially coherent beam from an incandescent lamp in a white-light Michelson interferometer. However we used a large-core multimode fiber to utilize as much light power as possible and to increase the signal-to-noise ratio even in the measurements of the interferograms of strongly light absorbing samples. By comparing the cross section of the cores between the two fibers, we see that we can utilize about  $10^3$  higher light power. The path length of one arm of the interferometer was modulated at  $f=1$  kHz by a piezoelectric actuator with the amplitude of  $\sim 250$  nm. The path length, or the delay time  $\tau$ , of the other arm was

<sup>a)</sup>Electronic mail: nakatsuk@bk.tsukuba.ac.jp

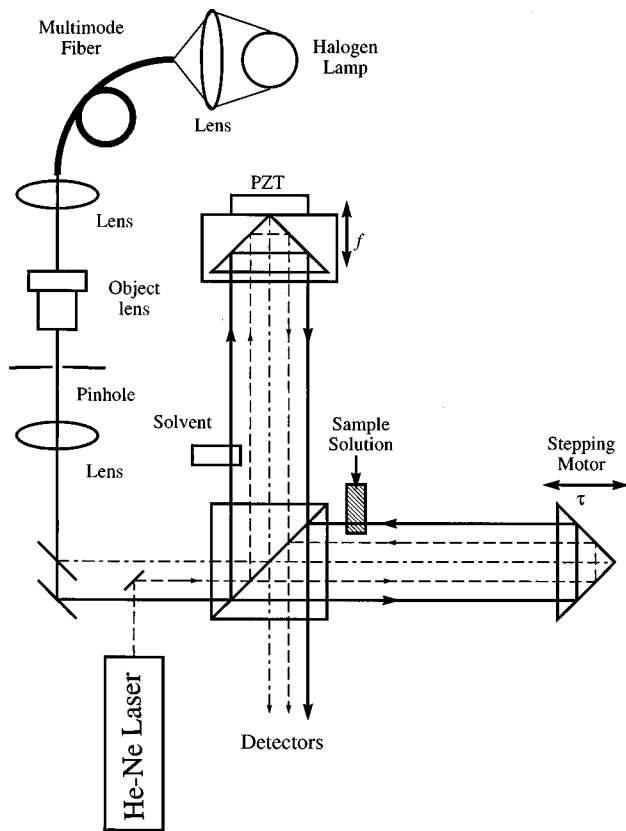


FIG. 1. Schematic diagram of the white-light Michelson interferometer.

changed by a corner-cube prism moved on a translation stage with a stepping motor. The output from the interferometer was detected by a photodetector and fed into a lock-in amplifier.

We measured two kinds of interferograms: one is the autocorrelation,  $C_A(\tau)$ , of the input light, and the other is the cross-correlation,  $C_C(\tau)$ , between the input light and the light transmitted through the sample. As is shown in Fig. 1, two other interferograms were simultaneously monitored with either of the two above-mentioned interferograms. One is the autocorrelation of the light from a He-Ne laser, and it was used for calibration of the path length. The other is that of the white light that did not path through the sample, and it was used to identify the position where path-length difference between the two arms is zero.

The autocorrelation interferogram  $C_A(\tau)$  is written as

$$C_A(\tau) = \langle E^*(t)E(t+\tau) \rangle, \quad (1)$$

where  $E(t)$  is the electric field of the white-light, and  $\langle \rangle$  denotes time average. In the linear response approximation, the electric field of the transmitted light,  $E'(t)$ , through the sample becomes

$$E'(t) = \int_{-\infty}^{\infty} dt' h(t-t')E(t'), \quad (2)$$

where  $h(t)$  is the response function of the sample. The cross-correlation interferogram,  $C_C(\tau)$ , between the input light,  $E(t)$ , and the output light,  $E'(t)$ , from the sample is written as

$$C_C(\tau) = \langle E^*(t)E'(t+\tau) \rangle. \quad (3)$$

If we insert Eq. (2) into Eq. (3),  $C_C(\tau)$  becomes

$$C_C(\tau) = \int_{-\infty}^{\infty} d\tau' h(\tau-\tau')C_A(\tau'). \quad (4)$$

By comparing Eqs. (2) and (4), we can say that if the wave form of the input light to the sample is the autocorrelation,  $C_A(\tau)$ , then the wave form of the output from the sample is the cross-correlation,  $C_C(\tau)$ . Therefore, in the linear regime we can predict the deformation of ultrashort light pulses by the propagation through samples by using a white-light Michelson interferometer.

On the other hand, Fourier analysis of the autocorrelation and cross-correlation interferograms gives us complex transmission coefficients of samples without relying on the Kramers-Kronig relation. By Fourier transformation of Eq. (2) we obtain

$$\tilde{h}(\omega) = \tilde{E}'(\omega)/\tilde{E}(\omega), \quad (5)$$

where  $\tilde{E}(\omega)$  and  $\tilde{E}'(\omega)$  are the Fourier transforms of the input field,  $E(t)$ , and the output field,  $E'(t)$ , respectively, and  $\tilde{h}(\omega)$  is the Fourier transform of the impulse response function,  $h(t)$ , and is called the complex transmission coefficient. The similar relation as Eq. (5) is obtained by the Fourier transformation of Eq. (4) as

$$\tilde{h}(\omega) = \tilde{C}_C(\omega)/\tilde{C}_A(\omega), \quad (6)$$

where  $\tilde{C}_A(\omega)$  and  $\tilde{C}_C(\omega)$  is the Fourier transforms of the autocorrelation,  $C_A(\tau)$ , and the cross-correlation,  $C_C(\tau)$ , respectively.

Because we measured the signal with a lock-in amplifier by using path-length modulation, our interferograms are not the autocorrelation or the cross-correlation in a strict sense. Both the autocorrelation and cross-correlation functions are modified from the true correlation functions in the same way as described by the following relation:

$$\tilde{C}'(\omega) = 2iJ_1\left(\frac{A\omega}{c}\right)\tilde{C}(\omega). \quad (7)$$

Here  $\tilde{C}(\omega)$  and  $\tilde{C}'(\omega)$  are the Fourier transforms of the true correlation and that of our interferogram, for either the autocorrelation or the cross correlation.  $J_1(A\omega/c)$  is the first-order Bessel function, where  $A$  is the path-length modulation amplitude and  $c$  is light velocity. Although the autocorrelation is an even function in general, the measured autocorrelation interferogram obtained in our system is an odd function. This is because the measured autocorrelation interferogram is multiplied by an odd function  $J_1(z)$  as is shown in Eq. (7). By using Eq. (7) we can get the relations for our interferograms as

$$C'_C(\tau) = \int_{-\infty}^{\infty} d\tau' h(\tau-\tau')C'_A(\tau'), \quad (8)$$

$$\tilde{h}(\omega) = \tilde{C}'_C(\omega)/\tilde{C}'_A(\omega), \quad (9)$$

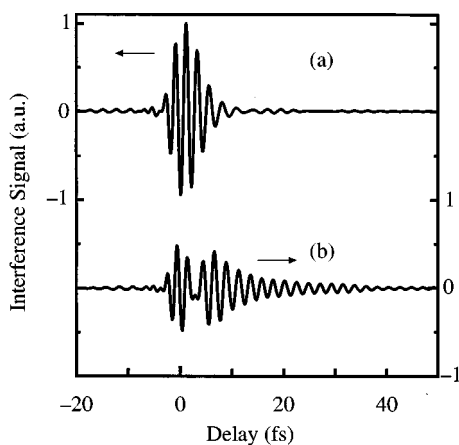


FIG. 2. (a) Autocorrelation and (b) cross correlation of oxazine 1 in methanol ( $1.2 \times 10^{-4}$  M).

which are exactly the same relations as Eqs. (4) and (6) for the true correlation functions. In this sense we can consider our interferogram as autocorrelation or cross correlation. For simplicity, we call the measured interferograms as the autocorrelation or the cross correlation in the following discussion.

The present lock-in detection by path-length modulation greatly increased the signal-to-noise ratio in the measurement of interferograms where the incident light is spatially incoherent and perfect interference between the beams from the two arms of the interferometer could not be obtained.

### III. EXPERIMENTAL RESULTS AND DISCUSSION

The sample we measured first was oxazine 1 dye molecules dissolved in methanol ( $1.2 \times 10^{-4}$  M). In the measurement of the autocorrelation the same type of glass cells (inner width 2 mm) containing only the solvent were inserted into both arms of the interferometer. We obtained the cross correlation by replacing the solvent in the glass cell in one arm of the interferometer with the sample solution. In this way, there was compensation for the change in the optical path length due to the glass cell and the solvent.

The autocorrelation and cross-correlation interferograms taken by the white-light Michelson interferometer are shown in Fig. 2. The Fourier transform of the autocorrelation interferogram is the power spectrum of the incident light to the interferometer, and it is shown in Fig. 3. The shorter-wavelength side was cut by the multimode optical fiber (Sumitomo Electric, MK-08) and the longer-wavelength side was cut by the sensitivity of the photomultiplier tube (Hamamatsu R955) used to detect the output light from the interferometer. More precisely the spectral profile shown in Fig. 3 or the Fourier transform of the autocorrelation is the total sensitivity profile of the white-light Michelson interferometer.

In the linear response regime, the relation between Eqs. (2) and (4) tells that if the wave form of the input light pulse to the sample solution is the autocorrelation interferogram shown in Fig. 2(a), then the wave form of the output from the sample is the cross-correlation interferogram shown in Fig. 2(b). In this way we can predict the deformation of light

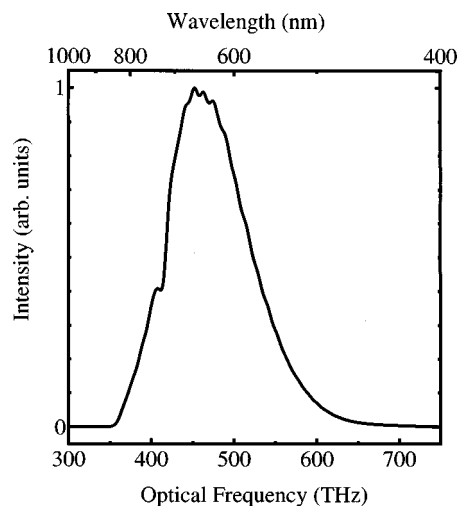


FIG. 3. Power spectrum of the incident light obtained by Fourier transformation of the autocorrelation in Fig. 2(a).

pulses through samples by using the white-light Michelson interferometer. The wave form of the output is explained as follows: The resonant incident light excites the oxazine 1 molecules to induce the coherent oscillation of the electric polarization. The light emitted from the polarization is out of phase by  $\pi$  with respect to the input light and interferes with the input light to reduce the amplitude of the transmitted light. After the input light pulse passes through, the induced polarization decays with its own decay time while emitting the free-induction decay signal. In this way, in the linear regime the precise wave form deformation of ultrashort light pulses can be shown by using the incoherent white-light Michelson interferometer.

Figure 4 shows the absorption spectrum and the spectrum of refractive index obtained by Fourier transformation of the measured interferograms. The agreement between the absorption spectrum thus obtained and that obtained with a conventional grating spectrometer is fairly good. The com-

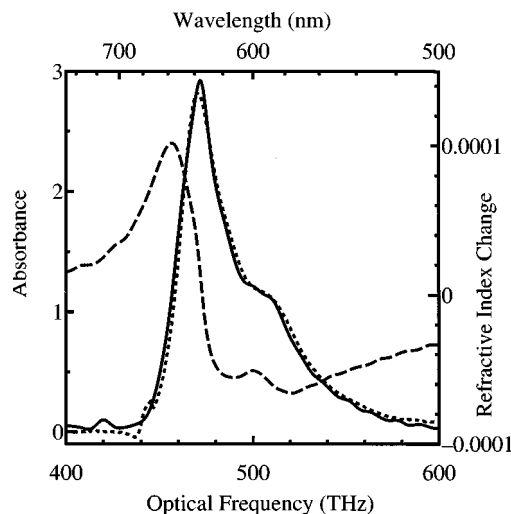


FIG. 4. Absorption spectrum (solid curve) and spectrum of refractive index (dashed curve) of oxazine 1 in methanol ( $1.2 \times 10^{-4}$  M) obtained from the measured interferograms. The absorption spectrum (dotted curve) obtained by using a conventional grating spectrometer is also shown.

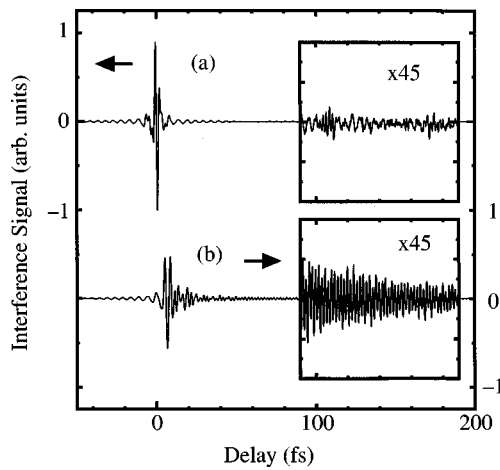


FIG. 5. (a) Autocorrelation and (b) cross correlation of the interference filter obtained by the white-light Michelson interferometer with the three detectors.

plex transmission coefficient of the sample was obtained by using the relation of Eq. (6) without relying on the Kramers–Kronig relation.

#### IV. EXTENSION OF THE SPECTRAL REGION

Next we tried to extend the sensitive spectral region of the white-light Michelson interferometer and increase the time resolution. The output light from the interferometer was split into three beams with two half mirrors. One beam was detected with a photomultiplier tube (Hamamatsu R955) which is sensitive in the visible region, and another beam was detected with a photomultiplier tube (Hamamatsu 7102) which is sensitive from 700 to 900 nm, and the other beam was detected with a germanium photodiode (Hamamatsu B1702-02) which is sensitive from 800 nm to 1.8  $\mu\text{m}$  in the near infrared region. The signals from the three detectors were added and fed into a lock-in amplifier. The autocorrelation interferogram of the incident light to the interferometer taken with this system is shown in Fig. 5(a). Now we can predict the wave form deformation of quasimonocycle pulses. The sensitive spectral region of the white-light Michelson interferometer is given by the Fourier transform of the quasimonocycle autocorrelation interferogram, and it is shown in Fig. 6. The long-wave side of the sensitive region extends more than 1.5  $\mu\text{m}$ . There is a sharp dip at around 1.4  $\mu\text{m}$ , which coincides with the absorption peak of water vapor or OH group. We tried to eliminate the dip at 1.4  $\mu\text{m}$  by substituting the ambient air of the interferometer with dry nitrogen gas. But the size of the dip did not change at all. It might be attributed to the residual absorption of optical components such as corner cube prisms or beam splitter cubes. The sharp structure in the sensitivity spectrum results in the long-lasting oscillation around the peak in the autocorrelation interferogram shown in Fig. 5(a).

In order to examine the performance of the white-light Michelson interferometer, as a test sample, we used an interference filter which has a transmission spectral profile extending from the visible region to the infrared region and at the same time has a sharp transmission peak. The cross-correlation interferogram taken by the interferometer is

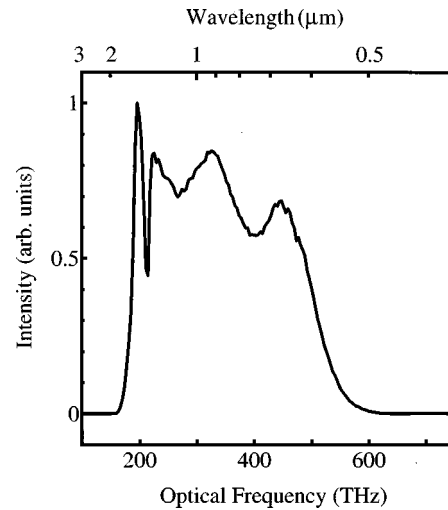


FIG. 6. Power spectrum of the incident light obtained by Fourier transformation of the autocorrelation in Fig. 5(a).

shown in Fig. 5(b). In this case also we can say that if the wave form of input light-pulse to the sample filter is the autocorrelation interferogram, then the wave form of the output from the filter is the cross-correlation interferogram. This relation holds precisely regardless of the sensitivity spectral profile of the interferometer. The transmission and phase spectra of the interference filter obtained by Fourier transformation of the measured interferograms are shown in Figs. 7(a) and 7(b), respectively. The transmission spectrum thus obtained agrees fairly well with that obtained by using a conventional grating spectrometer all through the sensitive region of the interferometer (Fig. 6). The long-lasting oscillation shown in the inset of Fig. 5(b) is attributed to the sharp transmission peak at 600 nm shown in Fig. 7(a).

#### V. CONCLUSION

We have shown that a spatially incoherent light source can be effectively used in white-light Michelson interferom-

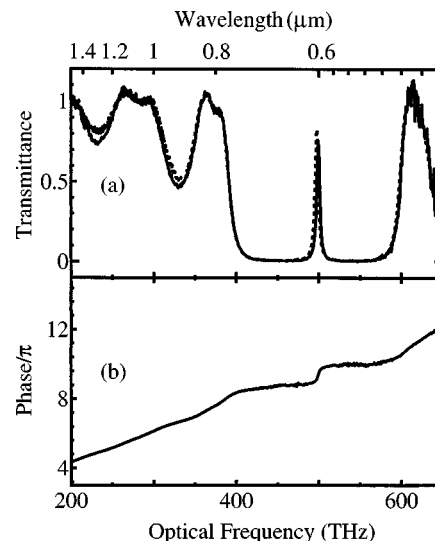


FIG. 7. (a) Transmission spectrum, and (b) phase spectrum of the interference filter obtained by Fourier transformation of the interferograms in Fig. 5. The dotted curve is the transmission spectrum obtained by using a conventional grating spectrometer.

eter to obtain the cross-correlation interferogram between the incident light and the transmitted light through samples in the visible and near infrared regions. In the linear regime we can predict the precise wave form deformation of ultrashort light pulses or even quasimonocycle pulses by the passage through samples and optical components. This information is very important for femtosecond laser technology and femtosecond spectroscopy. Moreover Fourier analysis of the interferograms gives the complex transmission coefficient without relying on the Kramers–Kronig relation.

- <sup>1</sup>W. H. Knox, N. M. Pearson, K. D. Li, and C. A. Hirlimann, *Opt. Lett.* **13**, 574 (1988).
- <sup>2</sup>K. Naganuma, K. Mogi, and H. Yamada, *Opt. Lett.* **15**, 393 (1990).
- <sup>3</sup>M. Beck and I. A. Walmsley, *Opt. Lett.* **15**, 492 (1990).
- <sup>4</sup>K. Naganuma and Y. Sakai, *Opt. Lett.* **19**, 487 (1994).
- <sup>5</sup>K. Naganuma, *Appl. Phys. Lett.* **64**, 261 (1994).
- <sup>6</sup>R. H. J. Kop and R. Sprik, *Rev. Sci. Instrum.* **66**, 5459 (1995).
- <sup>7</sup>S. Diddams and J.-C. Diels, *J. Opt. Soc. Am. B* **13**, 1120 (1996).
- <sup>8</sup>N. Tsurumachi, T. Fuji, S. Kawato, T. Hattori, and H. Nakatsuka, *Opt. Lett.* **19**, 1867 (1994).
- <sup>9</sup>T. Fuji, M. Miyata, S. Kawato, T. Hattori, and H. Nakatsuka, *J. Opt. Soc. Am. B* **14**, 1074 (1997).